6th International Conference on Advances in Experimental Structural Engineering
11th International Workshop on Advanced Smart Materials and Smart Structures Technology
August 1-2, 2015, University of Illinois, Urbana-Champaign, United States

Mode Identifiability of a Multi-Span Cable-Stayed Bridge Utilizing Stochastic Subspace Identification

Y. Goi[1], C.W. Kim[2]

1 *PhD student, Dept. of Civil and Earth Resources Engineering, Kyoto University, Kyoto 615-8540, Japan. E-mail: goi.yoshinao.38v@st.kyoto-u.ac.jp*
2 *Professor, Dept. of Civil and Earth Resources Engineering, Kyoto University, Kyoto 615-8540, Japan. E-mail: kim.chulwoo.5u@kyoto-u.ac.jp*

ABSTRACT
This study investigates the mode identifiability of a multi-span cable-stayed bridge in terms of a benchmark study utilizing stabilization diagrams of system model identified by means of the stochastic subspace identification (SSI). The cumulative contribution ratios (CCR) estimated from singular values of system model was also considered. Observations demonstrated that wind speed might influence to the mode identifiability of a specific mode of the cable-stayed bridge. Moreover the CCR estimated from the singular values of the system model showed that the time histories monitored during strong winds, such as typhoon, can be modeled with less system order than under weak winds.

KEYWORDS: *benchmark study, cable-stayed bridge, mode identifiability, cumulative contribution ratio, stabilization diagram.*

1. INTRODUCTION

How to manage aging civil infrastructure efficiently is a keen technical issue, and techniques of structural health monitoring (SHM) based on vibration measurements have been attracting bridge owners because of its feasibility of efficient inspection. Modal properties of bridges such as natural frequencies, damping ratios and mode shapes can be identified from vibration data of bridges, and changes in structural integrity lead to changes in these modal properties of the bridges (Zhang 2007, Kim et al. 2013). Thus vibration-based SHM is a useful technique if we can excite the bridge easily and effectively. There are two commonly ways to excite the bridges: forced vibration tests and ambient vibration tests. In the forced vibration test bridges are excited by a shaker, impact hammer, etc. On the other hand, the ambient vibration test utilizes various natural excitations such as wind, ground motions, etc. For the bridge health monitoring, an ambient vibration test is considered to be much more convenient than the forced vibration test as the natural excitations do not require traffic control while the forced vibration test requires traffic control during the test.

Various kinds of output only operational modal identification techniques based on ambient vibrations have been proposed (e.g. Heylen et al. 1997) by assuming natural excitations as stationary white noise inputs, and applied to monitor real bridges (e.g. Peeters et al. 2006, Kim and Chang 2014, Ni et al. 2015). An interesting observation on deficient modes whose identifiability depends on wind speed has been reported by Ni et al. (2015): the modal shape of the 2nd mode (deficient mode) of Ting Kau bridge which is a cable-stayed bridge is not identifiable under weak wind conditions while under typhoon condition it can be clearly identified. Prof. Y.Q. Ni of Hong Kong Polytechnic University proposed a benchmark study. In the benchmark study, 10 samples of "non-blind" bridge vibration data with information about wind speed and 6 samples of "blind" data without any other information are offered and investigations on the mode identifiability of the operational modal analysis methods are required. The main objectives of this benchmark study are:

1) To study the mechanism behind output-only modal identifiability, deficiency in modal identification, and criteria to evaluate robustness of the identified modes.
2) To apply and examine various methods of output-only modal identification.

This study aims to investigate a mechanism behind mode identifiability of the Ting Kau Bridge especially focusing on its linear system model. The stochastic subspace identification (SSI) (Overschee and Moor 1996) was considered. In this paper, only the non-blind vibration data are referred as the measurement data and considered

to investigate mode identifiability of Ting Kau Bridge.

2. INVESTIGATED BRIDGE AND BENCHMARK DATA

2.1. Ting Kau Bridge and Monitoring System

Ting Kau Bridge is a three-tower cable-stayed bridge with two main spans of 448m and 475m respectively, and two side spans of 127m each (Bergermann and Schlaich 1996). The bridge deck is separated into two carriageways with width of 18.8m each, and between them being three slender single-leg towers with heights of 170 m, 194 m, and 158 m, respectively. Each carriageway comprises two longitudinal steel girders along the deck edges with steel cross girders at 4.5 m intervals, and a concrete slab on top. The two carriageways with a 5.2 m gap are linked at 13.5 m intervals by connecting cross girders. The deck is supported by 384 stay cables in four cable planes. As part of a long-term SHM system devised by the Hong Kong Special Administrative Region (SAR) Government Highways Department, more than 230 sensors have been permanently installed on the TKB after completing the bridge construction in 1999 (Wong 2004, Ko and Ni 2005).

The layout of the sensors at eight deck sections on the Ting Kau Bridge is shown in Fig. 2.1. In each section, two accelerometers were installed on the east side and the west side of the longitudinal steel girders respectively to measure the vertical acceleration, and one accelerometer was installed on the central cross girder to measure the transverse acceleration. Fig. 2.2 illustrates the deployment of accelerometers on four deck sections of the Ting Kau Bridge. The sampling frequency of accelerometers was 25.6 Hz.

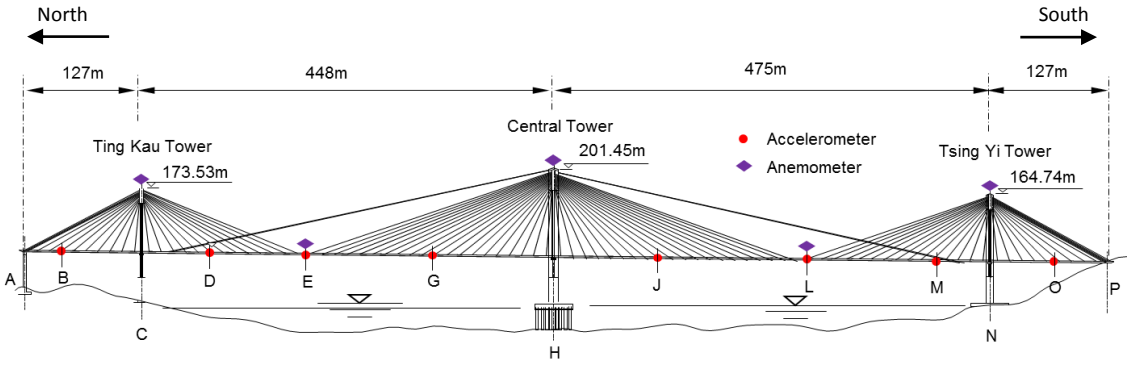

Figure 2.1 Deployment of accelerometers and anemometers on Ting Kau Bridge.

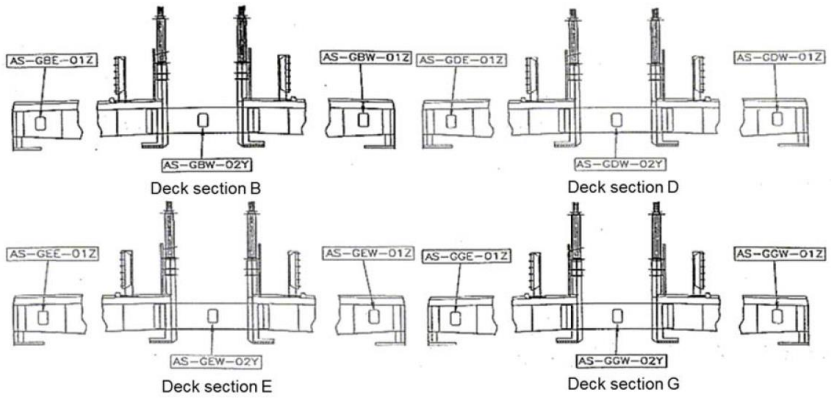

Figure 2.2 Deployment of accelerometers on four deck sections

2.2. Benchmark Data

For the benchmark study, 10 samples of non-blind measurement data are given. Table 2.1 shows the time duration

and the wind conditions of the measurement data. The data from Sample 1 to Sample 6 are measured under weak wind conditions and the data from Sample 7 to Sample 10 are measured under typhoon conditions. Traffic was blocked during the typhoons.

Table 2.1 Measurement data

Sample	Time duration	Mean hourly wind speed (m/s)	Remarks
Sample 1	15:00-16:00, 28 Dec 1999	2.00	
Sample 2	15:00-16:00, 18 Feb 1999	3.40	
Sample 3	15:00-16:00, 01 Mar 1999	3.34	
Sample 4	15:00-16:00, 21 Jun 1999	3.41	
Sample 5	15:00-16:00, 24 Jul 1999	6.17	
Sample 6	15:00-16:00, 12 Aug 1999	4.20	
Sample 7	03:00-04:00, 07 Jun 1999	12.11	Typhoon: Maggie
Sample 8	02:00-03:00, 23 Aug 1999	15.62	Typhoon: Sam
Sample 9	06:00-07:00, 16 Sep 1999	21.72	Typhoon: York
Sample 10	15:00-16:00, 16 Sep 1999	15.91	Typhoon: York

3. MODE IDENTIFICATION BY STOCHASTIC SUBSPACE IDENTIFICATION

3.1. Stochastic Subspace Identification

The dynamical system is modeled as following state space model (Heylen *et al*. 1997, Overschee and Moor 1996).

$$\begin{aligned}\mathbf{x}(k+1) &= \mathbf{A}\mathbf{x}(k) + \mathbf{w}(k)\\ \mathbf{y}(k) &= \mathbf{C}\mathbf{x}(k) + \mathbf{v}(k)\end{aligned} \tag{3.1}$$

where $\mathbf{x}(k)$ and $\mathbf{y}(k)$ denote the state of structure and measurement at each time step k respectively. $\mathbf{w}(k)$ and $\mathbf{v}(k)$ denote the process noise and measurement noise vectors respectively, and are assumed to be stationary white noise. System matrices **A** and **C** which contain the modal information are estimated by means of the least squares method for the minimal prediction error of state $\mathbf{x}(k)$ given by the forward Kalman filter. The poles of the dynamical system provide modal properties of the dynamical system.

The algorithms for the SSI is briefly described. Firstly, we obtain the oblique projection matrix $\boldsymbol{O}_i$ is estimated as following equation.

$$\boldsymbol{O}_i = \mathbf{Y}_\mathrm{f}\mathbf{Y}_\mathrm{p}^\mathrm{T}\left(\mathbf{Y}_\mathrm{p}\mathbf{Y}_\mathrm{p}^\mathrm{T}\right)^\dagger\mathbf{Y}_\mathrm{p} \tag{3.2}$$

where $(\cdot)^\dagger$ denotes Moore-Penrose pseudo inverse matrix. $\mathbf{Y}_\mathrm{f}$ and $\mathbf{Y}_\mathrm{p}$ are block Hankel matrices of the future and past outputs respectively and defined as follows.

$$\mathbf{Y}_\mathrm{p} = \begin{bmatrix} \mathbf{y}(0) & \mathbf{y}(1) & \dots & \mathbf{y}(j-1) \\ \dots & \dots & \dots & \dots \\ \mathbf{y}(i-2) & \mathbf{y}(i-1) & \dots & \mathbf{y}(i+j-3) \\ \mathbf{y}(i-1) & \mathbf{y}(i) & \dots & \mathbf{y}(i+j-2) \end{bmatrix} \tag{3.3}$$

$$\mathbf{Y}_\mathrm{f} = \begin{bmatrix} \mathbf{y}(i) & \mathbf{y}(i+1) & \dots & \mathbf{y}(i+j-1) \\ \dots & \dots & \dots & \dots \\ \mathbf{y}(2i-2) & \mathbf{y}(2i-1) & \dots & \mathbf{y}(2i+j-3) \\ \mathbf{y}(2i-1) & \mathbf{y}(2i) & \dots & \mathbf{y}(2i+j-2) \end{bmatrix} \tag{3.4}$$

The singular value decomposition (SVD) is then applied to factorize $\boldsymbol{O}_i$ as

$$\boldsymbol{O}_i = \mathbf{U}\mathbf{S}\mathbf{V}^\mathbf{T} = (\mathbf{U_1}\mathbf{U_2})\begin{pmatrix}\mathbf{S_1} & \mathbf{0}\\ \mathbf{0} & \mathbf{S_2}\end{pmatrix}(\mathbf{V_1}\mathbf{V_2})^\mathbf{T} \simeq \mathbf{U_1}\mathbf{S_1}\mathbf{V_1^T} \tag{3.5}$$

where $\mathbf{U}$ and $\mathbf{V}$ are unitary matrices with the appropriate size and $\mathbf{S}$ is a diagonal matrix with non-negative elements. The diagonal elements of $\mathbf{S}$ are known as singular values of $\boldsymbol{O}_i$. Singular values in $\mathbf{S}$ are listed in descending order. Therefore the components in $\mathbf{U_1 S_1 V_1^T}$ contain most of the information defining the elements in $\boldsymbol{O}_i$ and components in $\mathbf{U_2 S_2 V_2^T}$ are regarded as trivial components. Theoretically, the optimal state sequence $\mathbf{X}_i = [\mathbf{x}(i) \quad \mathbf{x}(i+1) \quad \dots \quad \mathbf{x}(i+j-1)]$ predicted by the Kalman filter in least square sense is obtained as follows.

$$\mathbf{X}_\mathrm{i} = \mathbf{S_1^{1/2} V_1^T} \tag{3.6}$$

The significant components of orthogonal vectors in the state sequence can be extracted by applying SVD to $\boldsymbol{O}_i$, and the system matrices are obtainable from $\mathbf{X}_i$. The number of poles corresponds to the number of singular values determined in Eq. 3.5. In other words, we can extract the significant modal components of the bridge from the measured acceleration data by the SVD.

3.2. Procedure for Mode Identification

In order to discuss the mode identifiability, this study utilizes stabilization diagrams (Heylen et al. 1997, Chang et al. 2013) to determine stable modes. The procedure for the mode identification adopted in this study is shown in Fig. 3.1, in which the maximum model order n=80 was decided to be the cumulative contribution ratio of singular values reaches 90% even in a noisy system which is discussed in Chapter 4. The frequency range of interest of TKB is below 0.5 Hz, and there is a concern about the modal identification below 0.5 Hz being interfered by higher-frequency information. This study adopted a decimation filter to avoid the effect of high frequency vibration. The lowpass Chebyshev type1 IIR filter of order 8 was used. In this study, modal characteristics of each model order were identified considering same size of the block Hankel matrix of measurement data, i.e. i =9 in Eq. 3.3 and Eq. 3.4.

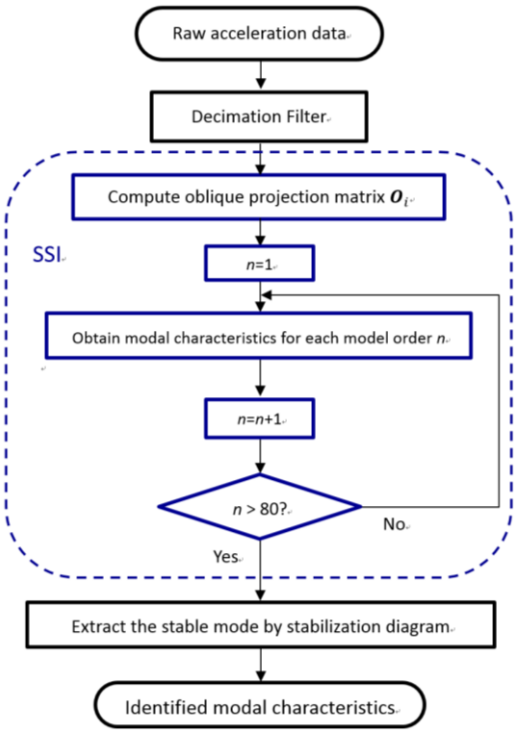

Figure 3.1 Modal identification procedure utilizing SSI

This study considered following stability criteria to extract stable modes.

$$\begin{gathered} \text{for } f_p: f_{p+\kappa} - f_\epsilon < f_p < f_{p+\kappa} + f_\epsilon \\ \text{for } \zeta_p: \zeta_{p+\kappa} - \zeta_\epsilon < \zeta_p < \zeta_{p+\kappa} + \zeta_\epsilon \\ \text{for } \psi_p: \mathrm{MAC}_l < \mathrm{MAC}_{(p,p+\kappa)} \\ (\kappa = -\kappa_\epsilon, \dots, -1, 1, \dots, \kappa_\epsilon) \end{gathered} \tag{3.7}$$

where, f_p, ζ_p, ψ_p are identified natural frequency, damping ratio and modal shape with model order p respectively. $\mathrm{MAC}_{(p,p+\kappa)}$ is modal assurance criterion (MAC) value between modal shape ψ_p and $\psi_{p+\kappa}$. The MAC value is estimated as bellow.

$$\mathrm{MAC}_{(p,p+\kappa)} = \frac{\left\|\psi_p^T \psi_{p+\kappa}\right\|^2}{\left\|\psi_p\right\|^2 \left\|\psi_{p+\kappa}\right\|^2} \tag{3.8}$$

where, parameters f_ϵ, ζ_ϵ, MAC_l in Eq. 3.7 are thresholds about tolerable range of variation of each modal property, and κ_ϵ is range of model order that evaluate the inequalities.

This study adopted a strict rule to extract stable modes: stable modes should satisfy all the criteria in Eq. 3.7. The thresholds adopted were $f_\epsilon = 0.002$ Hz, $\zeta_\epsilon = 0.5$ %, $\mathrm{MAC}_l = 0.8$ and $\kappa_\epsilon = 5$ in the frequency band lower than 0.5 Hz. The poles that have negative damping ratio were ignored.

4. MODE IDENTIFIABILITY

Natural frequencies, damping ratios and mode shapes of each measurement data are identified following the procedure described in Section 3.2. Identified natural frequencies are summarized in Table 4.1. A noteworthy point is that the modes with blanks (from Sample 1 to Sample 6 of the 2nd mode and from Sample 3 to Sample 7 of the 5th mode) in Table 4.1 indicate unstable modes, that is, the poles of these modes are too unstable to satisfy the stability criteria defined as Eq. 3.7 and are expelled from the identification. The identified results from the measurement data are comparable to the results reported in previous study (Ni *et al*. 2015), i.e. the 2nd mode (0.23 Hz) is not identified under the weak wind conditions.

Table 4.1 Identified natural frequencies.

Mode No	Natural frequency (Hz)									
	Weak Wind Condition						Typhoon Condition			
	Sample 1	Sample 2	Sample 3	Sample 4	Sample 5	Sample 6	Sample 7	Sample 8	Sample 9	Sample 10
1	0.162	0.162	0.162	0.163	0.163	0.164	0.167	0.164	0.165	0.165
2	-	-	-	-	-	-	0.227	0.227	0.227	0.226
3	0.256	0.256	0.258	0.257	0.258	0.260	0.263	0.264	0.257	0.260
4	0.286	0.286	0.284	0.286	0.282	0.282	0.289	0.292	0.287	0.289
5	0.292	0.292	-	-	-	-	-	0.297	0.300	0.300
6	0.307	0.310	0.308	0.315	0.312	0.318	0.323	0.324	0.319	0.317
7	0.358	0.364	0.360	0.358	0.357	0.358	0.362	0.361	0.359	0.359
8	0.372	0.373	0.374	0.372	0.372	0.374	0.374	0.373	0.373	0.373

Stabilization diagrams are also examined to find possible answers on the questions of the benchmark study. Fig. 4.1 shows the stabilization diagrams obtained from Sample 1 and Sample 7 which represent the weak wind condition and typhoon condition respectively. The stabilization diagram obtained under the weak wind conditions demonstrate that the 2nd mode (0.23 Hz) was not identified under weak wind conditions. This figure also shows that unstable poles are scattered widely in the frequency band below 0.23 Hz and no clear stable poles on the frequency of the 2nd mode (0.23 Hz) were observed. On the other hand, under typhoon conditions relatively less unstable poles were observed in the frequency band below 0.23 Hz. The typhoon conditions led to stable poles on the frequency of the 2nd mode. The above observations from the stabilization diagrams in Fig. 4.1 demonstrate that lower modes were easily contaminated by unknown noise under the weak wind conditions. However, under typhoon, structural modes were well excited and the system matrix will be dominated by structural information rather than noise, which might link with mode identifiability of the 2nd mode.

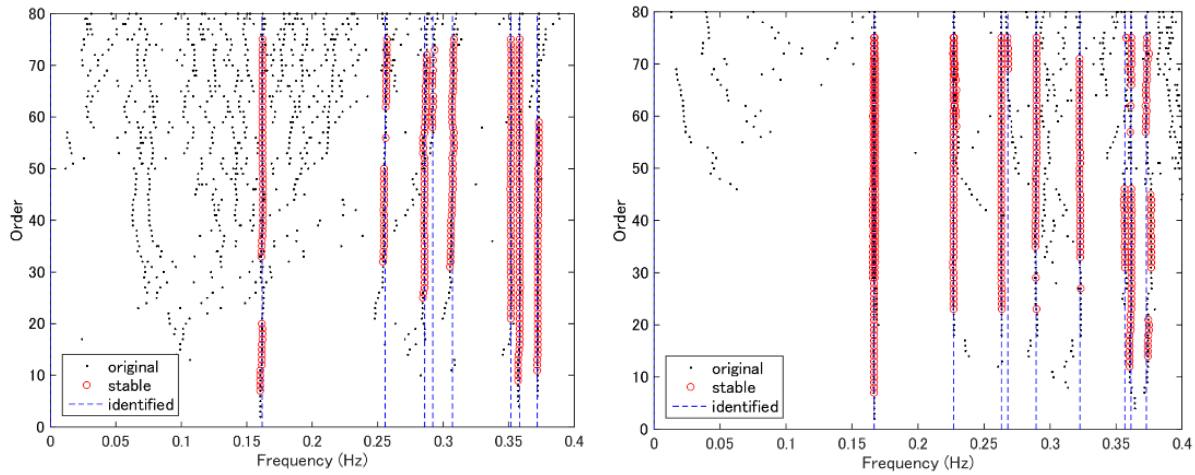

a) Weak wind condition (Sample 1)　　b) Typhoon condition (Sample 7)

Figure 4.1 Stabilization diagrams obtained from different wind conditions

The mean values of the power spectral density (PSD) of lateral accelerations for each sample are shown in Fig. 4.2, which shows that the measurement data in lateral directions under the weak wind conditions tend to be much exited in the low frequency band below 0.23Hz comparing with those under the typhoon conditions. Especially in the low frequency band below 0.18 Hz, most of the PSDs of the accelerations under the weak winds exceed the PSDs of the typhoon conditions, even though the exciting wind speed is weaker than typhoon conditions. One possible reason of weak wind conditions caused stronger PSDs than did the typhoon below the frequency range of 0.18 Hz may be any influence of traffic since traffic were controlled during the typhoon.

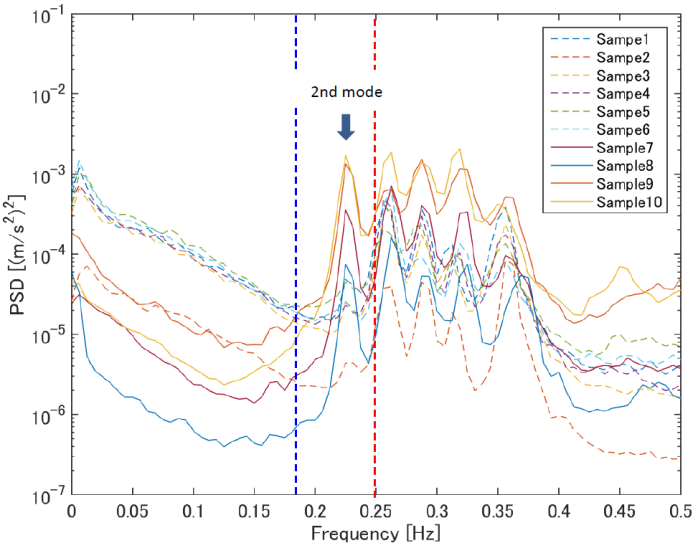

Figure 4.2 Mean value of lateral acceleration PSD

To investigate difference of identified systems under different wind conditions, the cumulative contribution ratio (CCR) of singular values of the system is considered. The CCR of model order *n* is defined as Eq. 4.1.

$$CCR = \frac{\sum_{i=1}^{n} s_i}{\sum_{i=1}^{N} s_i} \tag{4.1}$$

where, s_i is the *i*-th singular value in Eq. 3.5 and *N* is the total number of the singular values. The CCR estimated from all the measurement data is plotted with respect to the model order as shown in Fig. 4.3, which demonstrated that typhoon conditions resulted in higher CCR than the weak wind conditions. In other words, in considering same model order, the CCR under typhoon conditions comprises more information about the system than those under weak wind conditions. Therefore, vibrations of the bridge under typhoon conditions can be modeled by the

dynamic system with lower model order. For example, a system model containing the 90% of the measurement information can be described by the model order of 50 under the typhoon conditions. On the other hand it needs the model order of 80 to contain 90% of the system information under the weak wind conditions (see vertical broken lines in Fig. 4.3). That is, the 2nd mode can be well excited to be identified as a stable mode under typhoon conditions.

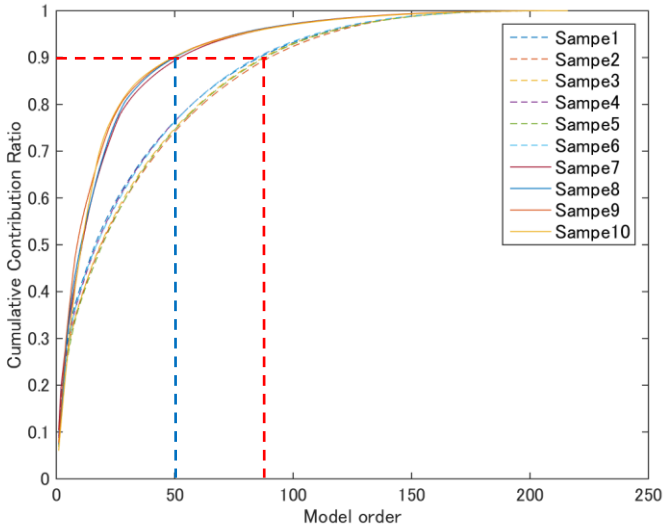

Figure 4.3 Cumulative contribution ratios of singular values calculated in SSI

5. CONCLUDING REMARKS

The mode identifiability of Ting Kau Bridge which is a multi-span cable-stayed bridge under different wind conditions was investigated as a benchmark study. The stochastic subspace identification (SSI) was applied to identify mode properties. Stabilization diagrams of given measurement data were examined to extract stable modes. Cumulative contribution ratio (CCR) estimated from singular values of the identified system model is also adopted to investigate the contribution of poles of the estimated system models to the dynamical behavior of the structure under different wind conditions.

Identified natural frequencies from the measurement data were well comparable to the existing study. That is, existence of deficient 2nd mode whose identifiability depends on the wind conditions was observed.

The stabilization diagrams of data measured under weak wind conditions showed widely scattered unstable poles in the frequency band below 0.23 Hz but no clear stable poles on the frequency of the 2nd mode (0.23 Hz) was observed. On the other hand, under typhoon conditions less unstable poles were observed in the frequency band below 0.23 Hz and stable poles were observed on the frequency of the 2nd mode. In other words, it can be said that lower modes might be easily contaminated by unknown noise under the weak wind conditions. However, under typhoon, structural modes were well excited and the system matrix will be dominated by structural information rather than noise, which might link with mode identifiability of the 2nd mode.

Observations from PSD curves of lateral acceleration showed that, especially in the low frequency band below 0.18 Hz, most of the PSDs of the lateral accelerations under the weak winds exceed the PSDs of the typhoon conditions, even though the exciting wind speed is less than typhoon conditions. One possible reason of appearing stronger PSDs under weak wind conditions than under the typhoon below the frequency range of 0.18 Hz may be any influence of traffic since traffic were controlled during the typhoon.

Observations also demonstrated that the CCR reaches higher ratio with less model order under typhoon conditions in comparison to the condition under weak wind. This implies that the 2nd mode under the typhoon conditions is excited enough to be identified as the stable mode. Feasibility of utilizing the CCR of singular values of the system model to investigate performance of mode identification was shown.

The observations of stability diagrams, PSD and CCR implied the existence of unknown noise which disturb the stable identification of the modal characteristics under the weak wind conditions. Next step for this study is to investigate influence of the traffic and cable vibrations to mode identifiability.

AKCNOWLEDGEMENT

The authors would like to thank Prof. Y.Q. Ni of Hong Kong Polytechnic University for providing monitoring data and materials relevant to the Ting Kau Bridge and organizing the benchmark study. The authors also would like to thank Prof. H. Shirato of Kyoto University for his valuable comments on cable-stayed bridges and cable vibrations.

REFERENCES

1. Bergermann, R. and Schlaich, M. (1996), Ting Kau Bridge, Hong Kong, *Struct. Eng. Int.*, **6:3**, 152-154.
2. Brincker, R., Zhang, L. and Andersen, P. (2000), Modal identification from ambient response using frequency domain decomposition, *IMAC XVIII*, San Antonio, USA.
3. Chang, K.C., Kim, C.W. and Kitauchi, S. (2013), Stability diagram aided multivariate AR analysis for identifying the modal parameters of al steel truss bridge subjected to artificial damage, *Proc. of the 13th East Asia-Pacific Conf. on Structural Eng. and Constr. (EASEC-13)*, Sapporo, Japan.
4. Deraemaeker, A., Reynders, E., De Roeck, G. and Kullaa, J. (2007), Vibration-based structural health monitoring using output-only measurements under changing environment, *Mechanical Systems and Signal Processing*, **22:1**, 34-56.
5. He, X. and De Roeck, G. (1997), System identification of mechanical structures by a high-order multivariate autoregressive model, *Computers and Structures*, **64:1-4**, 341-351.
6. Heylen, W., Lammens, S. and Sas, P. (1997), Modal Analysis Theory and Testing, K.U.Leuven.
7. Kim, C. W., Isemoto, R., Sugiura, K. and Kawatani, M. (2013), Structural Fault Detection of Bridges based on Linear System Parameter and MTS Method, *J. of JSCE*, **1:1**, 32-43.
8. Kim, C.W. and Chang, K.C. (2014), A Field Experiment on a Simply Supported Steel Truss Bridge for Damage Detection Utilizing Statistical Patterns of Identified Modal Parameters, *Proc. of the 4th Int. Symp. On Life-Cycle Civil Eng.*, Tokyo, Japan.
9. Ko, J.M. and Ni, Y.Q. (2005), Technology developments in structural health monitoring of large-scale bridges, *Eng. Struct.*, **27:12**, 1715-1725.
10. Ni, Y.Q., Wang, Y.W. and Xia, Y.X. (2015), Investigation of mode identifiability of a cable-stayed bridge: comparison from ambient vibration responses and from typhoon-induced dynamic responses, *Smart Struct. Syst.*, **15:2**, 447-468.
11. Peeters, B., Dammekens, F., Magalhaes, F., Van der Auweraer, H., and Cunha, A. (2006), Multi-run Operational Modal analysis of the Guadiana Cable-stayed Bridge, *Proc. of IMAC24*, St. Louis, USA.
12. Van Overschee, P. and De Moor, B (1996), Subspace Identification for Linear Systems, Kluwer Academic Publishers.
13. Wenzel, H. and Pichler, D. (2006), Ambient Vibration Monitoring, John Wiley & Sons.
14. Wong, K.Y. (2004), Instrumentation and health monitoring of cable-supported bridges, *Struct. Control Health Monit.*, **11:2**, 91-124.
15. Zhang, Q. W., (2007), Statistical damage identification for bridges using ambient vibration data, *Computers and Structures*, **85:7-8**, 476-485.